

We are IntechOpen, the world's leading publisher of Open Access books Built by scientists, for scientists

4,800

Open access books available

122,000

International authors and editors

135M

Downloads

Our authors are among the

154

Countries delivered to

TOP 1%

most cited scientists

12.2%

Contributors from top 500 universities



WEB OF SCIENCE™

Selection of our books indexed in the Book Citation Index
in Web of Science™ Core Collection (BKCI)

Interested in publishing with us?
Contact book.department@intechopen.com

Numbers displayed above are based on latest data collected.
For more information visit www.intechopen.com



Recent Advances in Two-Photon Stereolithography

Arnaud Spangenberg, Nelly Hobeika,
Fabrice Stehlin, Jean-Pierre Malval, Fernand Wieder,
Prem Prabhakaran, Patrice Baldeck and
Olivier Soppera

Additional information is available at the end of the chapter

<http://dx.doi.org/10.5772/56165>

1. Introduction

Recent developments in nanoscience and nanotechnology were strongly supported by significant advances in nanofabrication. The growing demand for the fabrication of nano-structured materials has become increasingly important because of the ever-decreasing dimensions of various devices, including those used in electronics, optics, photonics, biology, electrochemistry, and electromechanics (Henzie et al., 2004; Fan et al., 2006). In particular, a societal revolution is expected with the miniaturization of mechanical, chemical or biological systems known as microelectromechanical systems (MEMS) (Lee et al. 2012), or micrototal analysis systems (μ TAS) (Reyes et al. 2002, Dittrich et al. 2006, West et al. 2008).

Among all fabrication processes, photolithography has been strongly developed since few decades to fulfil to the needs of the microelectronics industry. Researches in this area were essentially motivated by finding ways to provide new solutions to pursue the trend towards a constant decrease of the size of the transistors as stated in the "Moore's law" (Moore, 1965). To reach these objectives, lithographic fabrication methods have been widely diversified leading to DUV lithography (Ridaoui et al., 2010), X-ray lithography (Im et al., 2009) and e-beam lithography (Gonsalves et al. 2009) to quote a few. Although some of these techniques exhibit resolution of less than 10 nm, these methods are inherently 2D. Unlike conventional microelectronics components, many MEMS or μ TAS devices (motors, pumps, valves...) require 3D fabrication capability to insure the same function as the corresponding macroscopic device. Thus, lithographic fabrication of 3D microstructures has emerged and has been divided in two categories depending if they give access to restricted or arbitrary 3D pattern fabrication. On the first hand, specific structures as periodic patterns have been made using self-assembly

(Shevchenko et al. 2002), layer-by-layer assembly (Kovacs et al. 1998), soft lithography (Quake et al. 2000), and holographic photopolymerization (Campbell et al. 2000). However by these techniques, no free-moving or complex microstructures have been achieved. On the other hand, arbitrary 3D patterns have been realized by using the so-called direct write technologies which gathers ink-based writing (Lewis et al. 2004), microstereolithography (Maruo et al. 2002) and two-photon stereolithography (TPS) (Kawata et al. 2001; Maruo et al. 1997). Though examples of submicrometer resolution have been demonstrated for ink-based writing (Lewis et al. 2004) and microstereolithography (Maruo et al. 2002), these techniques are mainly used for micro or macrofabrication.

In this context, two-photon stereolithography which is an advanced version of microstereolithography appears of high interest since it offers intrinsically sub-100 nm resolution. Additionally to its unique ability of writing arbitrary structures with sub-100 nm features without use of any mask, TPS is also an attractive fabrication process due to the versatility of materials used including polymers, biopolymers, ceramics, metals, and hybrid materials.

The aim of this chapter is to review some recent works about two-photon stereolithography and its applications. In the first part, a brief introduction to TPS and the fundamental concepts will allow illustrating its interest and its current development. The second part will be dedicated to the most relevant materials developed for TPS regarding to the applications targeted. Furthermore, some typical applications where 3 dimensionalities play a crucial role will be highlighted. Finally, the last part will describe the recent advances in TPS both from the writing speed and the resolution (Li et al. 2009) in order to compete with other nanofabrication techniques. As the result, the contribution of this chapter is to propose a comprehensive overview of fundamental issues in TPS as well as its current and future promising potential.

2. Two-photon stereolithography

2.1. Introduction

One of the first attempts to fabricate 3D structures arised from IBM in 1969 (Cerrina, 1997). By combining electrodeposition and X-ray lithography, high-aspect ratio metal structures were obtained. Further works on X-ray lithography gave rise to the well-known process LIGA in the early 1980s (Becker et al. 1984). Despite the maturity of the technique and demonstration of some 3D complex structures, their application has not been widespread due to the availability of synchrotron radiation sources and X-ray masks.

Historically speaking, TPS began with the 3D microfabrication process using photopolymers developed by Kodama in 1981 (Kodama, 1981). Further developments lead to the birth of stereolithography, then microstereolithography to achieve resolution down to 1 μm . Even if in some cases, submicrometer resolution has been demonstrated (Maruo et al. 2002), it is still challenging to obtain microstructures with nano or submicron features due to the layer-by-layer nature of this technique. To overcome this drawback, Wu et al. (Wu et al. 1992) proposed the two-photon lithography concept which is based on the nonlinear optical process of two

photon absorption (TPA). This work was directly inspired of the first demonstration of localized excitation in two-photon fluorescence microscopy by Denk et al. two years before (Denk et al. 1990). However, the feasibility of TPS¹ as a real 3D fabrication technique was illustrated by Maruo et al. in 1997 through the fabrication of a 7 μm -diameter and 50 μm -long spiral coil (Maruo et al. 1997). Finally, in 2001, micromachines and microbull with feature sizes close to the diffraction limit were realized (Kawata et al. 2001). By using non-linear effects of TPS, subdiffraction-limit spatial resolution of 120 nanometers has been successfully achieved.

2.2. Two-photon absorption

Contrary to conventional stereolithography techniques where polymerization is induced by absorption of a single photon, TPS is based on two photon absorption (TPA) process. TPA and more generally multiphoton absorption (MPA) process have been first predicted in 1931 by Marie Goeppert-Mayer (Goeppert-Mayer, 1931) and then verified experimentally thirty years later (Kaiser et al. 1961), thanks to the advent of laser. Finally, two-photon photopolymerization was experimentally reported for the first time in 1965 as the first example of multiphoton excitation-induced photochemical reactions (Pao et al. 1965). However, it's only with the commercialization of tunable solide ultrashort pulse laser like Ti:Sapphire laser in the 1990s that application of TPA is widespread in various domains like biology imaging (two photon fluorescence microscopy) or microfabrication (TPS).

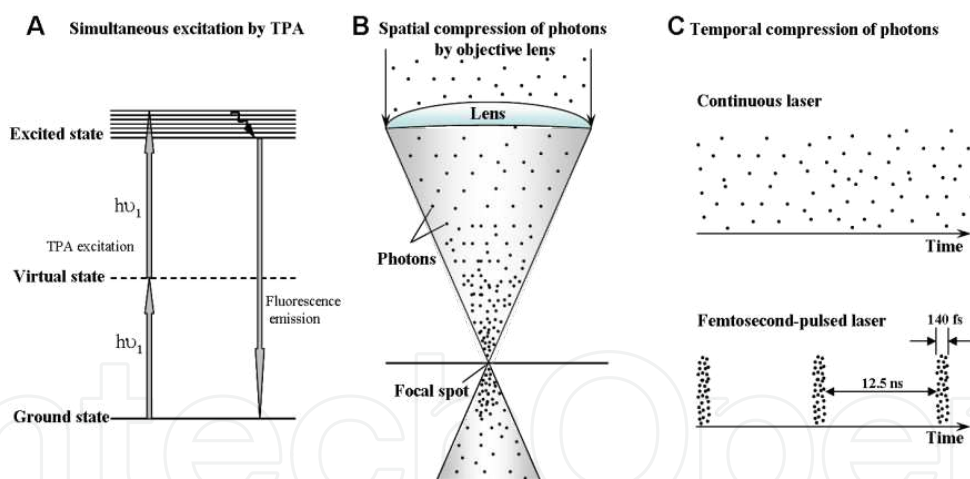


Figure 1. A. Mechanism of TPA when simultaneous excitation occurs. B and C. Illustration of two methods for increasing the probability that TPA occurs: density of photon is increased by B. spatial compression using objectives with high numerical aperture, C. temporal compression using ultrafast lasers.

Two different mechanisms have been described for TPA: the sequential excitation and the simultaneous two-photon excitation. In the frame of TPS, only the second one is involved (Figure 1A). In this case, a virtual intermediate state is created by interaction of the material with the first absorbed photon. In order to reach the first real excited state, a second photon

¹ TPS is also called two-photon polymerization (TPP), multiphoton absorption polymerization (MAP), 3-dimensional Direct Laser Writing (3D DLW) or 3-dimensional lithography.

has to be absorbed during the short lifetime (around 10^{-15} s) of this virtual state. To increase the probability of such a non-linear absorption process, high density of photons is requested. Consequently, in main applications (including TPS) where TPA is involved, objectives with high numerical aperture (NA) and ultra short pulse laser are employed for increasing spatial and temporal density of photons, respectively (Figure 1B and C). The main interest of TPA compared to single photon absorption is that excitation is localized within the focal volume of a laser beam. Consequently, it gives access to 3D microfabrication since the polymerization threshold is not reached out of the focal volume. Typically, volume less than $1\text{ }\mu\text{m}^3$ can be addressed. In parallel to the technical developments for TPA, molecular engineering has been strongly developed to design molecules or molecular architectures with large TPA cross section. An exhaustive review on this point can be found in reference (He et al. 2008) and few typical examples will be given in the next section.

2.3. Experimental set-up for TPS

The typical TPS setup is composed of three main parts: (i) the excitation source, (ii) the computer-aided design (CAD) system and (iii) the scan method. The excitation source with high intensity is important to favor TPA process. Even if Ti:Sapphire laser operating at 800 nm are often used, Baldeck and coworkers have demonstrated that TPS could be performed successfully by using a cheap Nd-YAG microlaser operating at 532 nm (Wang et al. 2002). The CAD system has to be chosen carefully since trajectories can influence the writing time and more important the mechanical resistance of the final structure. Finally, the scan method will have a crucial impact of the throughput of the writing process. The first possibility is to use Galvano mirrors for horizontal scanning coupled to piezoelectronic stage for vertical scanning which presents the advantage to scan with high speed. However, the total horizontal range accessible by this optical system is limited to few ten of micrometers due to spherical aberration when using objectives with high numerical aperture. The most popular solution consists to scan in x, y and z direction by using a piezoelectric stage. While the scan speed is low compared to previous option, few hundred of micrometer can be scanned.

As depicted in Figure 2, a typical set-up is composed of a mode-locked Ti:Sapphire laser as excitation source which presents duration pulse of ten hundred of femtosecond at 800 nm, repetition rate around 80 MHz and average output power of 1-3 W. The intensity of the laser is controlled by an optical or mechanical shutter. Before the introduction of the beam into the microscope, it is expanded so as to overfill the back aperture of the objective. By tightly focusing the pulsed laser beam (ns to fs pulses) into a multi-photon absorbing material, it is possible to trigger a photoreaction (e.g. photopolymerization) inside a volume below the dimension of the voxel. Complex structures (such as in Figures 3, 4, 6 and 8) can then be generated by moving in the laser focus in the 3 dimensions inside the monomer substrate. Usually, samples are placed on a 3D piezoelectric stage, and then move above the fixed laser beam by CAD. Upon the irradiation, only areas exposed at the focal point are polymerized further than the polymerization threshold, leading to the desired structures after washing away the unsolidified photoresist. Finally, the back reflection is collected by an additional port and send to a CCD to monitor the fabrication in real time.

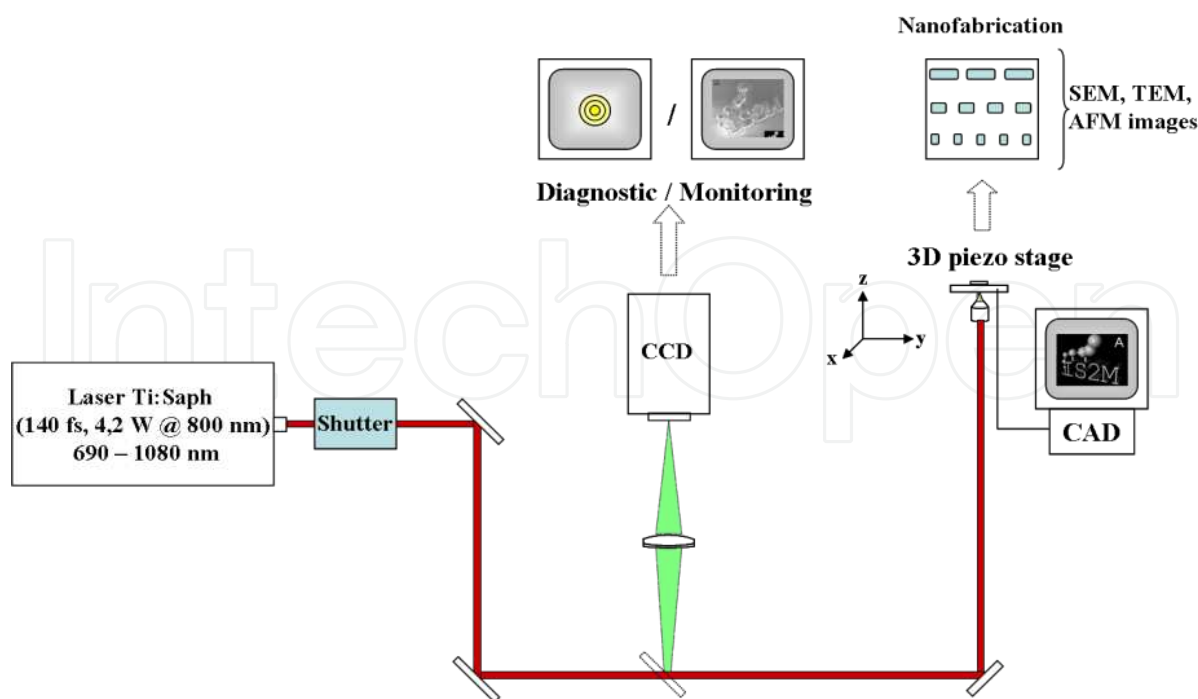


Figure 2. Schematic typical experimental TPS set-up.

3. Materials for two-photon stereolithography

Basically, the formulation destined to TPS is composed of 2 main components: a photoinitiator system and a monomer. The two-photon photoinitiator is a species, or a combination of chemicals able to absorb efficiently two photons to generate excited states from which reactive species can be created. One of the most important parameter is the two-photon absorption cross section that directly characterizes the capacity of the photoinitiator to absorb two photons. The reactive species (radicals or ions) must be able to initiate polymerization of the monomers that constitute the building blocks of the final material. After initiation, propagation and termination reactions take place as observed in the sequences of classical polymerization scheme.

In principle, any one-photon photopolymerizable system can be adapted to TPS, provided that a suitable TPS photoinitiator can be added to the monomer system. Most of the published works deal with free radical photopolymers. The main reason is relative to a wider availability of free radical photoinitiators.

Additionally to the photoinitiator and monomers, other chemicals can be added in TPS systems like inhibitors (to control the polymerization threshold and thus spatial extend of polymerization - some examples will be given in the next section), and additives to bring specific properties (fluorophores, metal nanoparticles, quantum dots, etc...). The choice of the monomer is in relation with the final application whereas the choice of the photoinitiator integrates the irradiation wavelength and nature of the monomer.

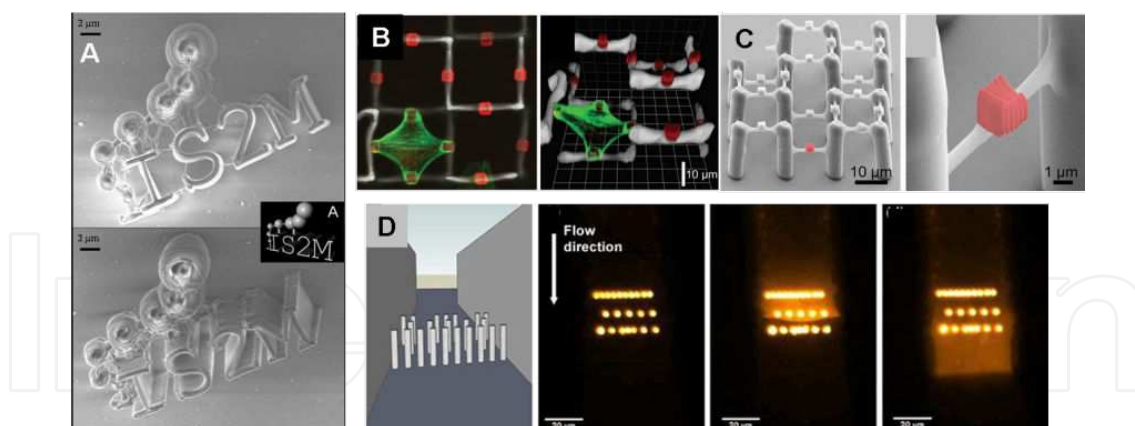


Figure 3. structures realized by TPS with A. polyacrylate derivatives (λ_{exc} : 532 nm; average power : 20 μW ; writing speed: 45 $\mu\text{m.s}^{-1}$; Malval et al. 2011), B. and C. sol-gel materials for biocompatible 3D scaffold (λ_{exc} : 808 nm; average power : 20 mW; writing speed: 200 $\mu\text{m.s}^{-1}$ Klein et al. 2011), D. trypsin derivative for biocatalysis degradation (λ_{exc} : 532 nm; average power : 1 mW; writing speed: nc, losin et al. 2012). Reproduced from the respective references.

As illustrated in Figure 3, different examples of 3D structures have been realized with various materials. Interest of such structure will be discussed in each corresponding material subsection. The next paragraphs are aimed at giving some examples of systems and associated applications.

3.1. Free-radical photoresists

Among different monomers available, acrylate monomers have been the most widely used for TPS. The reason for this success is a wide range of commercially available acrylate monomers with tailored properties: chain length, number of reactive function, viscosity, polarity to quote a few. Moreover, acrylate monomers exhibit a high reactivity and good mechanical properties that allow complex 3D structures being created.

In parallel, a wide choice of free-radical TPP photoinitiators has been developed. Highly efficient two-photon absorbing systems such as 4,4'-dialkylamino trans-stilbene (Cumpston et al. 1999) and other bis-donor bis(styryl)benzene or bis(phenyl)polyene (Lu et al. 2004; Zhang et al. 2005; Rumi et al. 2000) were employed for two-photon initiated free radical polymerization. Other conjugated photoinitiators as fluorenes (Belfield et al. 2000; Martineau et al. 2002, Jin et al. 2008) and ketocoumarins (Li et al. 2007) derivatives also demonstrated remarkable TPS properties. Finally, another promising strategy is the direct photogeneration of highly reactive radicals such as α -aminoalkyl ones.

In particular, Malval et al. demonstrated an elegant strategy to improve the efficiency of thioxanthone-based systems (Malval et al. 2011, Figure 3A). New hybrid anthracene-thioxanthone system assembled into a chevron-shaped molecular architecture was proposed. A strong increase in the two-photon absorption cross section by more than a factor of 30 as compared to thioxanthone was observed. As a consequence, anthracene-thioxanthone constitutes a suitable two-photon initiating chromophore with a much higher efficiency as thioxanthone used as reference. At $\lambda_{\text{exc}} = 710$ nm for instance, the two-photon polymerization threshold of

anthracene-thioxanthone was shown to be five times lower with respect to that of thioxanthone.

Additional examples of polyacrylate structures realized by TPS can be found in figure 4 section 4.1.

3.2. Cationic photoresist

Cationic photoinitiated polymerization of epoxides, vinyl ethers and methylenedioxolanes has received increasing attention, owing in large part to the oxygen insensitivity of the cationic process (Belfield et al. 1997a and 1997b). Moreover, cationic photoresist appears as an interesting choice from application point of view since UV negative tone photoresists have demonstrated their interest for microelectronics, optics, microfluidic or MEMS.

However, the difficulty to design efficient TPA photoacid generators has limited the development of TPA cationic photoresists. For this reasons, many efforts have been devoted to increase the sensitivity of such systems. First approach was based on sensitizers such as coumarin (Li et al. 2001), phenothiazine (Billone et al. 2009), or thioxanthone (Steidl et al. 2009) associated to a commercial PAG such as onium salts. Second approach relies on a molecular association of the acid generator functionality into the structure of the two-photon active chromophore. In the latest case, the reactivity of the PAG is no longer limited by diffusion and thus a significant improvement of the photopolymerization efficiency was demonstrated (Zhou et al. 2002; Yanez et al. 2009; Xia et al. 2012).

Among other application, the epoxy-based photoresists are extremely interesting when complex structures with high aspect ratio are needed. Indeed, thanks to their good mechanical properties, they have been successfully used for application in microfluidic (Maruo et al. 2006) or MEMS (Bückmann et al. 2012).

3.3. Advanced functional materials

Despite their advantages, polymers have intrinsic limitations for some applications. For instance, their mechanical properties at high temperature or in contact with solvents degrade rapidly. They also present low refractive index that limits their use in optical applications. Their toxicity may prevent them from use in contact with living organisms. For these reasons, alternative strategies have been developed to combine the advantages of 3D structuration by TPA and functional materials.

The sol-gel route is interesting in the frame of micro-nano-fabrication since it allows the fabrication of inorganic or hybrid organic-inorganic materials at relatively low temperature. The first strategy followed for combining lithography and sol-gel materials consisted in developing hybrid precursors that can undergo both sol-gel hydrolysis-condensation reaction and photoinduced crosslinking (Blanc et al. 1999; Soppera et al. 2001). These materials, also called Ormocer® or Ormorsil® have been adapted to TPA by use of suitable photoinitiators and interesting applications in the frame of optics (Ovsianikov et al. 2008) or biology (Klein et al. 2011, see Figure 3B, C) were demonstrated. These materials were mostly used in optics since

the refractive index of the material can be tuned by adding metal alcoxides. However, in these hybrid materials, the proportion of organic moieties in the crosslinked material is still important, so many efforts have been dedicated to the formulation of fully inorganic materials (Passinger et al. 2007).

Another important class of inorganic materials is metals. Metals nanoparticles, nanostructures or thin layers are indeed very interesting for electrical connections in devices and also for their plasmonic properties. Recent works have been reported on the fabrication of 3D metallic structures by combining TPS and silver evaporation (Rill et al. 2008). However, by this process, full metal coverage is challenging and induces a supplementary step. Therefore, several groups have developed more direct strategies based only on TPS. For instance, Prasad et al. have fabricated submicrometric plasmonic structures which exhibit interesting conductive properties (Shukla et al. 2011). More recently, Spangenberg et al. also demonstrated that a silver complexe can be used as TPA photoinitiating system and as precursors for nanoparticles fabrications, leading in a single step to a polymer-metal nanoparticles nanocomposite (Spangenberg et al. 2012). Such routes open the doors towards microstructures with conductive properties or magnetic properties that can be useful for MEMS actuation.

One other very important and growing field of applications for TPA materials is relative to biological applications. TPA microstructuring has been extensively used the last years to propose micro and nanostructured surfaces with tailored chemical composition to be used as model substrates to investigate the development of biofilms. The unique advantage of TPS is to propose real 3D structures that mimic with more accuracy the local environment of cells or bacteria than planar surfaces. In this context, polymer matrixes have been widely used but also, sol-gel materials were proposed since they are biocompatbile materials that can be used as inert topological matrixes, as illustrated in Figure 3B and 3C (Klein et al. 2011). Additionally, biological materials like trypsin or collagen precursors were developed to propose a direct writing route for 3D biocompatible structures. Besides the interest of allowing a direct writing of complex structures, an advantage of TPA microfabrication is to be adapted for integration of microstructures in closed environment. For example, Iosin et al. demonstrated the possibility of integrating trypsin's micropillars in a microfluidic system (Figure 3D). Trypsin is an enzyme used for catalyze the degradation of specific peptide. Interestingly, by following the variation of fluorescence intensity resulting from the peptide clivage, the authors have shown that trypsin structures kept its enzyme catalysis activity.

Although numerous materials have been designed to fulfill the requirements of various applications, there is still an important demand for optimizing current systems. Besides, with the emergence of STED-like lithography (for STimulated Emission Depletion, see next section), designs of new photosystems will be crucial for the development of such technique.

4. Current challenges in TPS

As shown through several examples, TPS is a powerful and attractive technique for present and futures applications. Due to the need of a well-controlled 3D nanofabrication technique,

several commercial set-ups have emerged on the market since 5 years. However TPS suffers from two main drawbacks for a more largely widespread in other scientific area or in industries. The first roadblock concerns the low-throughput of the process. Indeed, TPS is based on a serial process (i.e. point-by-point writing) which is a serious problem when mass production is needed. Moreover, compared to low-throughput techniques like e-beam lithography, resolution achievable by TPS is still 1 or 2 order of magnitude lower.

In this section, we will discuss about different approaches to address these specific points and highlight some recent developments which answer mostly to these drawbacks and promise a brilliant future to TPS.

4.1. Resolution

Because of the rapid improvement of TPS resolution in the past decade, a special attention has to be care on the way to define and measure it. In the most of works, “resolution” corresponds to the lateral and/or axial features size of single voxel or single line. Different methods such as ascending scan method (Sun et al. 2002) or suspending bridge method (DeVoe et al. 2003) have been proposed in order to improve the accuracy of the measurements. However, these two methods suffer from drawbacks which are the difficulty to avoid the truncation effect and the unknown influence of material’s shrinkage. Therefore, though less information is provided, most of the groups define resolution as the width of a single line on the surface.

Nevertheless, with the emergence of several STED-like lithographies, more precise definition of resolution has become necessary in order to compare their abilities. Although extension of the famous Abbe’s criterion introduced in conventional or two-photon absorption microscopy can be extended to TPS to describe the optical limitation of the lithography system, ultimate resolution for a given optical lithography system has to be determined by considering the role of the photopolymer. Indeed, in the frame of the writing of two close lines, due to consumption of photoinitiators and diffusion of various species (photoinitiator, scavengers), the writing process of the second line can be strongly affected. This effect is sometimes referred as the resin’s memory. Thus strong dependence with respect to the initial concentrations of photoinitiator as well as the viscosity of the matrix is expected. Up to date, no mathematical model includes all the parameters. Therefore, as suggested by Fischer et al. (Fischer et al. 2012), a better solution for determine both axial and lateral resolution would be the fabrication of a 3D periodic unit as a crystal photonic for a given photopolymerizable system. It has to be mentioned that typical ratio between axial over lateral resolution in TPS is ranging from 2 to 5 depending of optical conditions. In the next part, one has to keep in mind that the resolution or feature size is given for both an optical and chemical system.

4.1.1. Overview of the different strategies

Since the microbull with 120 nm features size realized by Kawata and coworkers (Kawata et al. 2001), various approaches have been attempted to improve the resolution of TPS (Figure 4). The first approach which is still used nowadays relies on the design of high-efficiency photoinitiators. By this method, linewidths of 80 nm have been measured (Xing et al. 2007).

Another approach based on the use of a shorter wavelength has allowed writing of 3D structure with 60 nm feature size (Haske et al. 2007). Indeed, as dictated by the extended to TPS Abbe's criterion, lateral resolution is proportional to the wavelength. However, the wavelength can not be reduced indefinitely since the material may absorb linearly at shorter wavelength and consequently lead to the lost of the intrinsic resolution of TPS. Finally, more recent and impressive feature size was obtained by an enhanced version of TPS inspired by STED microscopy (Li et al. 2009). The principle of this technique will be described in detail in the next section. With 800 nm excitation wavelength, voxel of 40 nm height have been achieved, that represents $\lambda/20$. This spectacular result has to be compared with the voxel of 600 nm height obtained by using conventional TPS where excitation wavelength is set at 800 nm which corresponds to $\lambda/1.33$. Even if no experimental evidence has been shown for lateral resolution by this technique, $\lambda/20$ is also clearly achievable. Further insight of this new technique is addressed in the next subsection.

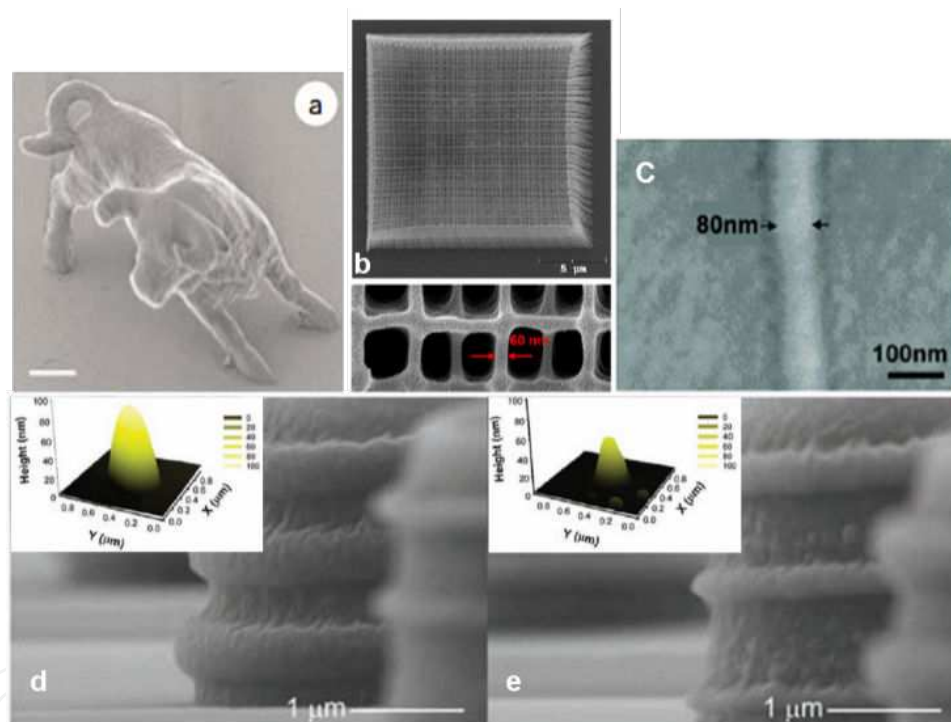


Figure 4. Improving spatial resolution of two-photon microfabrication by different strategies during the past decade. a) the famous microbull exhibiting 120 nm features size due to intrinsic properties of TPS ($\lambda = 780$ nm, $\lambda/6.5$; Kawata et al. 2001), b) Photonic crystal with 60 nm features size due to the use of shorter wavelength ($\lambda = 532$ nm, $\lambda/8$; Haske et al. 2007), c) 80 nm linewidth by using a high efficient photoinitiator ($\lambda = 800$ nm, $\lambda/10$; Xing et al. 2007), d) and e) microtower fabricated by using a conventional TPS and a STED-like TPS, respectively. In d and e insets, AFM measurements of voxel size are shown. e) inset is the current smallest axial resolution (40 nm) for a voxel thanks to a STED-like method ($\lambda = 800$ nm, $\lambda/20$; Li et al. 2009). Reproduced from the respective references.

4.1.2. STED-like lithography

In the recent past, the diffraction resolution barrier of fluorescence light microscopy has been radically overcome by stimulated emission depletion (STED) microscopy. Since its theoretic-

cally (Hell et al. 1994) and experimentally (Klar et al. 1999) birth, STED delivers nowadays routinely images of biological samples with a resolution down to 10-20 nm. Due to its great achievements in life-science, STED and more globally super resolution microscopy have been recognized as the “method of the year” in 2008 in Nature Methods. Finally, world record lateral resolution down to 5.6 nm using visible light has been reported by Hell’s group (Rittweger et al. 2009). In STED, a first short laser pulse is used to bring fluorescent molecules in their excited state. In order to de-excite these chromophores through stimulated emission, a second laser pulse (usually at longer wavelength to avoid one photon absorption) has to occur after vibrational relaxation of the excited electronic state but before fluorescence occurs i.e. few ps to few ns later than the first laser pulse. The efficiency of the deactivation strongly depends on the intensity and the wavelength of the depletion pulse, as well as the time delay of depletion pulse versus the excitation pulse. The precise localization of fluorescence arises from the spatial phase shaping of the depletion beam. The latter causes de-excitation to occur everywhere except in a region at the center of the original focal volume. The idea to translate these groundbreaking concepts to optical lithography has been evoked in 2003 (Hell et al. 2003), but first demonstration applied to TPS has been published only 6 years later (Li et al. 2009). Nowadays, in the frame of STED-like optical lithography, 3 different depletion mechanisms have been reported in the literature. In all cases, two laser beams are used, one for excitation and a second one for deactivation as illustrated in Figure 5. Whereas the excitation beam allows the formation of species (i.e radicals) which initiate the polymerization, the phase shaped deactivation beam allow photophysically or photochemically inhibition of the reticulation around the central excited zone. Depending of the phase mask used, the voxel can be reduced along the axial direction (bottle-beam shape, see Figure 5B) or along the lateral direction (donut shape).

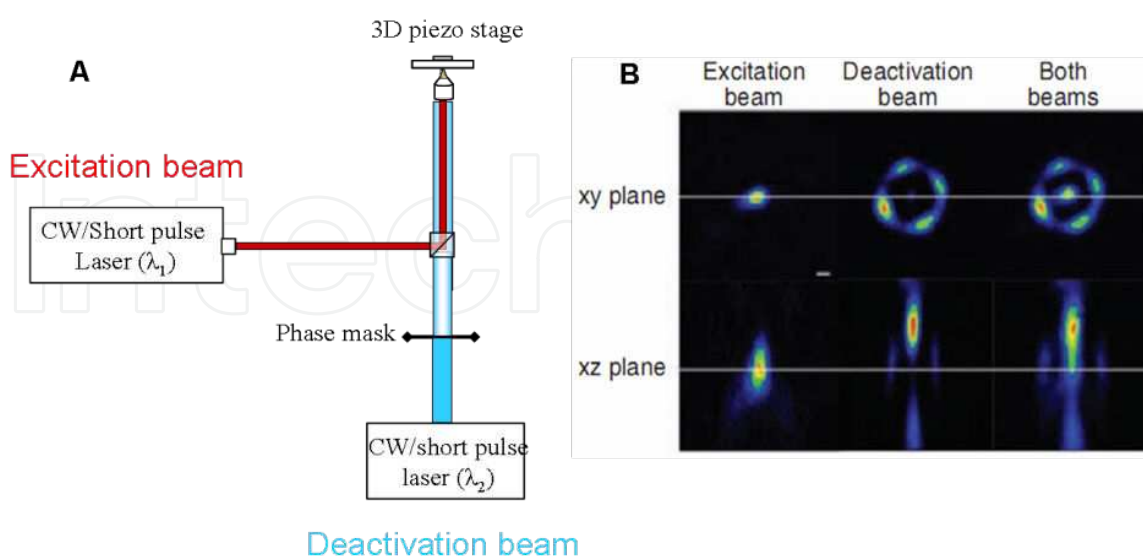


Figure 5. A. Schematic experimental set-up for STED-like optical lithographies. B. False-color, multiphoton-absorption-induced luminescence images of the cubes of the PSFs of the excitation beam, the phase shaped deactivation beam, and both beams together. Adapted from reference (Li et al. 2009).

4.1.2.1. Two-color photoinitiation/inhibition lithography

Among the three STED-like optical lithography methods, the so called two-color photoinitiation / inhibition lithography (2PII) is the only one based on a *photochemical* deactivation of photoinitiator (Scott et al. 2009, McLeod et al. 2010). In this case, by using continuous laser, the excitation is performed by a single photon absorption process at 473 nm and deactivation occurs also by a linear process at a distinct wavelength (364 nm). Upon deactivation beam, two weakly reactive radicals are produced which can interact with the initiating radical to stop the polymerization. By using a donut mode for shaping the deactivation beam, reduction of the lateral extent of single voxel until 65 nm is reached. More recently, with a similar set-up, another group has claimed having designed a more efficiency photopolymerizable system which has been illustrated by the fabrication of 40 nm dots (Cao et al. 2011). While the idea to use inexpensive continuous laser sources is attractive, this process has been demonstrated only for fabrication of 2 dimensional structures. Although manipulation of the photoinhibiting wavelength into a "bottle beam" profile would induce confinement along the third axis, when focusing deeper into the photoresist volume, both excitation and deactivation might be attenuated by the linear absorption of the material. Besides, consumption of photoinitiator and/or photoinhibitor along the pathway of the beam could lead to a time and space dependence of concentration of photoactivable species during the 3D fabrication. 2PII based on two-photon absorption process for both excitation and deactivation could avoid this problem, but up to now, no such experiment has been reported in the literature.

4.1.2.2. RAPID lithography

The first attempt to translate the spectacular optical resolution from STED microscopy to lithography has to be attributed to Fourkas's group (Li et al. 2009). Contrary to 2PII, deactivation is based on a *photophysical* process. On preliminary experiments, Fourkas and coworkers have used the conventional STED configuration. In this case, the excitation beam (800 nm) was overlaid by a second beam red-shifted with respect to the excitation beam wavelength. Then, in order to enhance the efficiency of stimulated emission, the depletion pulse was stretched to duration of 50 ps. to guarantee enough intensity of the depletion beam. Deactivation i.e. inhibition of the polymerization was observed for a wide range of wavelength (760 to 840 nm). However, whereas tuning the pulse delay from 0 to 13 ns between the two beams should affect the efficiency of the inhibition, no significant effect had been observed. Consequently the deactivation was not assigned to stimulated emission like in STED, but the authors have ascribed this effect to the depletion of an intermediate state with longer lifetime. Therefore they have decided to name this method RAPID for Resolution Augmentation through Photo-Induced Deactivation. Further experiments are under investigation to determine the nature of the intermediate specie.

Thanks to the longer lifetime of the intermediate, a second configuration has been successfully used: depletion effect has been performed with continuous laser which cancel the need to control the delay between excitation (800 nm) and depletion (800 nm) beams. By using the later configuration and a bottle beam profile for the depletion beam, voxels of 40 nm height have been achieved. In the frame of this study, the depletion effect is so

sensitive that the excitation beam can induce itself the deactivation. Interestingly, for a RAPID compatible photoinitiator, the linewidth increases at faster scan speed. In the opposite, in conventional photoinitiator, faster scan and consequently weaker exposure dose yields to decrease of the linewidth. This opposite effect for RAPID photoinitiator is explained by the depletion effect done by the excitation beam. Indeed, slow down the scan speed allow to excited photoinitiator to be deactivate. Smartly, the authors have taken benefit of this unexpected dependence towards scan speed to propose system insensitive to abrupt change of trajectory (Figure 6). In this case, photopolymerizable system combines both conventional and RAPID photoinitiators. Finally, according to conclusions of Wegener and coworkers (Fischer et al. 2012), because the depletion time-constant is between 15 and 350 ms in case of RAPID lithography, writing speed is comprised between $30 \mu\text{m.s}^{-1}$ to $150 \mu\text{m.s}^{-1}$. While this speed corresponds to typical speeds used in academic field, this slow speed might be an obstacle for its use in industry (see section 4.2).

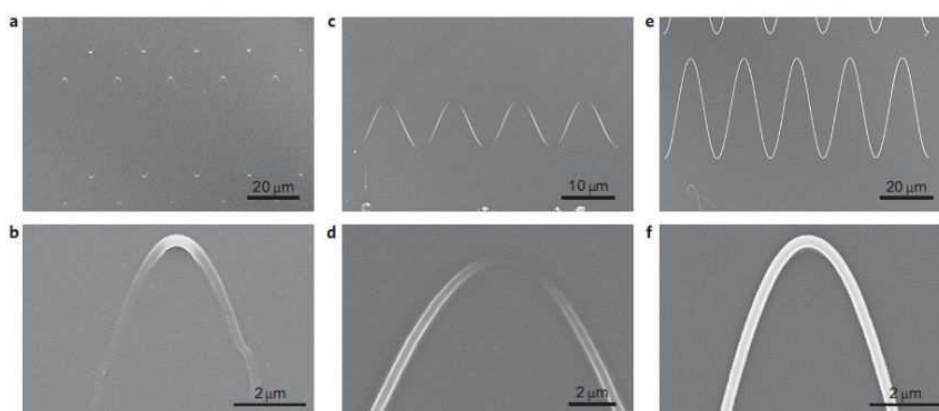


Figure 6. A, B Large and close view of fabrication of sinusoidal structures with a conventional photoinitiator, respectively. C, D Large and close view of fabrication of sinusoidal structures with a RAPID photoinitiator, respectively. E, F Large and close view of fabrication of sinusoidal structures with a mixture of conventional and RAPID photoinitiators, respectively. Reproduced from reference (Stocker et al. 2010).

4.1.2.3. STED lithography

For efficient STED, molecules have to present large oscillator strength between the ground state S_0 and the first excited state S_1 to favor later depletion. Because of their use in fluorescence microscopy, such type of molecules has also to exhibit strong fluorescence quantum yield. But this relatively long lifetime excited state (usually few ns) allows the depletion to take place.

In contrary, common photoinitiator exhibit low oscillator strength and are designed to present efficient intersystem crossing (ISC) yielding to reactive species which can give rise to radical and further to polymerization. Moreover, excited state lifetime of photoinitiator is usually found to be around 100 ps which would result in the use of high power pulses shorter than 100 ps to induce depletion. Unfortunately, with this large pulse energy, depletion could be competed by multiphoton absorption leading to undesired polymerization. Compare to previous STED-like lithography technique, STED lithography requires the use of two distinct-

wavelength short pulse lasers for both excitation and deactivation. In addition, pulse delay between the two beams has to be controlled carefully. While this configuration seems more constraining than 2PII and RAPID, higher scan speed (around 5 m.s^{-1}) is expected (Fischer et al. 2012).

STED lithography experiment has been attempted with isopropylthioxantone (ITX) as a photoinitiator. But further experiments such as pump-probe experiment have shown that the STED mechanism was not the main depletion pathway (Wolf et al. 2011) as claimed in previous work (Fischer et al. 2010). Based on the pump-probe experiment in ethanol (Wolf et al. 2011), a better suitable candidate appears to be the dye (7-diethylamino-3-thenoylcoumarin) (DETC) since stimulated emission was clearly demonstrated.

However, because the S_1 lifetime of a molecule usually depends on the solvent, a detailed and adapted pump probe study of DETC in the monomer has been realized (Fischer et al; 2012). While it has been shown that stimulated emission was not the only possible pathway, it was the first clear evidence of the possibility to perform true STED lithography. Fast and slow components of depletion were observed to exhibit opposite wavelength dependencies which indicate the existence of two distinct depletion mechanisms (Figure 7A). The fast component was ascribed to stimulated emission depletion, since its spectral dependence fits nicely the spectrum of the stimulated-emission (SE) cross-section. The slow component was not assigned in the frame of this study and further studies have to be accomplished to unravel this point. It has to be noted that at longer wavelength the relative strength of the fast component is weak regarding those of slow component.

Interestingly, STED lithography pump-probe experiment with the same photopolymerizable system, but with a depletion wavelength set at 642 nm has been performed by Harke and coworkers (Harke et al. 2012). In this experiment, pulse delay experiment has been realized, but no evidence of STED has been observed. Nevertheless, the unique component of depletion effect presents a timescale in the same range as typical triplet lifetime. The authors assume that the depleted excited state is not the singlet state S_1 as in STED, but the triplet state T_1 . Besides, one possible and well-known pathway to deplete the triplet state proposed by the authors is the reverse intersystem crossing (ReISC).

Until now, only 3 pump-probe experiments have been performed by two distinct groups. Even if these studies lead to different observations and conclusions, it can certainly be explained by the use of different experimental conditions (depletion wavelength, pulse delay, excitation wavelength). Thus results illustrate the need to improve the knowledge in STED-like lithography process to define requirements list for efficient STED lithography photoinitiators.

The recent progresses of STED-like lithography have allowed new very promising applications in photonics. 3D polarization-independent carpet cloak for visible light have been fabricated for the first time which demonstrate the unique ability of TPS as 3D fabrication method (Fischer et al. 2011). In this case, 3D photonic crystal exhibits distance between two lines of 375 nm and 175 nm in axial and lateral directions, respectively. This has to be compared with the 510 and 210 nm values found in the frame of conventional TPS for axial and lateral directions, respectively. Whereas noticeable improvement has been shown for axial resolution,

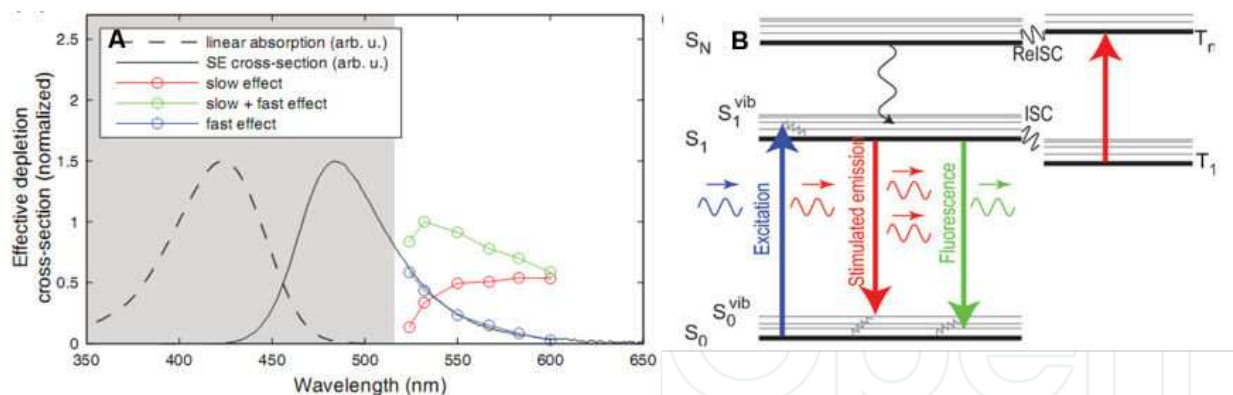


Figure 7. A. Spectral sensitivity of the different processes for 10 mW depletion power. Due to pronounced single photon absorption, depletion is not possible in grey area. B. schematic illustration of the different pathway involved in the depletion of DETC. Reproduced from references (Fischer et al. 2012 and Harke et al. 2012).

the gain in lateral resolution is less remarkable. This is explained by the use of a bottleneck beam shaping for the depletion beam. While combination of bottleneck and donut phase masks could be used to shape the beam and so to improve simultaneously lateral and axial resolution, it may be interested for specific applications to use only bottleneck beam since it can induce a more spherical voxel (ratio of 2.1 in this example).

Owing to its current and unique fabrication ability and its potential ability regarding to high-throughput (5 m.s⁻¹ scan have been predicted for pure STED lithography), an exponential increase of works on this becoming hot topic is expected in the near future.

To conclude about these STED-like section, it has to be mentioned that because of the relative novelty of STED-like optical lithographies (since 2009) and the fact that until now only 5 groups in the world have shown their skills to design such type of experiment, new insights are expected to appear rapidly in the near future. Interdisciplinary research has to be lead in order to propose a STED lithographic set-up with the dedicated optimized materials for few tens of nanometers in three dimensions. This will give birth of the first 3D arbitrary nanofabrication technique.

4.1.3. Diffusion-assisted TPS

An alternative method to improve the resolution is to add a quencher in the photopolymerizable system. In presence of quencher, the photoinduced radical can be quenched which consequently prevents polymerization. By this way, it has been shown that the radical diffusion can be controlled resulting in the confinement of the polymerization region (Tanaka et al. 2005). However, in this reported work, the concentration of quenching molecules has to be much larger than those of radical produced in order to result in an effective deactivation. Therefore, Lu and coworkers designed a novel photoinitiator with a radical quenching moiety (Lu et al. 2011). In this case, an intramolecular radical deactivation can occur leading to a more efficiently control of radical diffusion than in the case of an intermolecular one. As a result, finer features can be formed. However, by these methods no sub-diffraction gaps between two lines have been demonstrated, and only small effects on the feature size have been observed.

More recently, Sakellari and coworkers proposed another route to control the extent of the polymerization region (Sakellari et al. 2012). From their point of view, since a nondiffusing quencher results only in an increase of the polymerization threshold, they proposed to add a mobile quencher. Contrary to other works (Tanaka et al. 2005, Lu et al. 2011) where the quencher plays its inhibitor role by interacting with the photoinitiator or the generated radical, the quencher used in this work is an amine-based monomer. It interacts with other monomer or become part of the polymer backbone without compromising the mechanical stability of the structure. Last but not least, the amine functions allow a future metallization or further chemical functionalization. By this method, fabrication of woodpile structures with 400 nm intralayer period has been achieved for the first time with a *single beam* (Figure 8). Without the amine-based monomer, the authors have already shown in previous works that the minimum intralayer period achievable for an equivalent crystal photonic was around 900 nm (Sun et al. 2010). Moreover, this 400 nm intralayer period obtain by diffusion method has to be compare with the best result obtained by STED-like lithography, i.e. 375 nm intralayer period for the same type of photonic crystal (Fischer et al. 2011). Interestingly, while a single beam is used in the frame of this diffusion assisted high resolution TPS (as named by their authors), comparable resolution are obtained in both cases. While this method is easier to implement in laboratory compare to STED-like lithography, it has to be mentioned that in order to get such impressive resolution, the scan speed is intrinsically low to allow diffusion of the quencher into the scanned area. Typical scan speed in this study is around $20 \mu\text{m.s}^{-1}$. In the last section, solutions to overcome this speed limitation will be addressed.

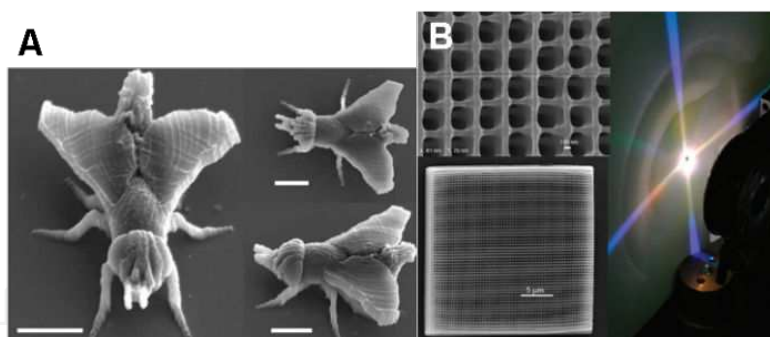


Figure 8. A. Microstructures realized by intramolecular quenching method. Scale bars are $5 \mu\text{m}$. B. SEM images of photonic crystal fabricated by diffusion assisted high resolution TPS and diffraction pattern generated by the photonic device. Reproduced from references (λ_{exc} : 780 nm; average power : 7.70 mW; writing speed: $66 \mu\text{m.s}^{-1}$, Lu et al 2011) and (λ_{exc} : 800 nm; average power : 20 mW; writing speed: $20 \mu\text{m.s}^{-1}$ Sakellari et al. 2012), respectively.

4.1.4. Other methods

Recently, 40 nm feature size has been obtained by combining chemical and optical approaches (Emons et al. 2012). The measurement of feature size has been performed by suspending bridge method. From a chemical point of view, the authors have demonstrated that the addition of a crosslinker (pentacrylate derivative) allow a resolution enhancement of a factor 2 (150 nm feature size versus 82.5 nm with a 50 fs pulse laser). As expected, the addition of crosslinker

should play a positive effect on the resolution since it allow to the suspended line to be maintained during the development step. In the other hand, an additional resolution enhancement has been achieved by using shorter laser pulse: the use of 8 fs instead of 50 fs allows improving feature size of the line from 150 nm to 90 nm for photoresin without cross linker.

In addition to the above optical and chemical tricks, further improvement of resolution can be achieved by other minor technical development like high hybrid optics diffractive (Burmeister et al. 2012).

To conclude, recent technical developments of TPS open the doors to strong improvement of the resolution. Even if the diffraction limit has been beaten both in lateral and axial direction thanks to different methods such as the STED-like lithography or the diffusion-assisted high resolution TPS, effort research has to be focus on new photopolymerizable system to benefit completely of the intrinsic resolution achievable by the different techniques. For STED-like lithography, optimization of the photopolymerizable system should lead to feature size around 10 nm. Finally, when comparing the different technique, a particular attention has to be taken into account concerning the maximum scan speed for future use in industry. This will be the object of the next section.

4.2. Recent advances in throughput: From prototyping towards production of semi-series

Despite the possibilities to fabricate 3D objects with sub-100 nm features in a single step, TPS use is as far as we know limited to scientific community. Indeed, owing to the point-by-point writing process, TPS appears as an extremely slow technique for mass production in industry. Typical writing speed range in academic research goes from few $\mu\text{m.s}^{-1}$ to few mm.s^{-1} which has to be compared with the few m.s^{-1} used in industry for different laser process (ablation, laser control, rapid prototyping by inspired-stereolithography methods,...). Until 2003, as for resolution, the research effort for increasing the throughput of TPS was mainly focused to the synthesis of high-efficiency photoinitiators. Nevertheless, in the past decade several research groups have proposed various strategies to break down this technological bolt.

4.2.1. Influence of the scanning mode

As an attempt to solve this problem, Sun et al. demonstrated the impact of the laser beam trajectory over the manufacturing time by significantly increasing the fabrication efficiency of 90% when using CSM (contour scanning method, also called vector mode) mode rather than RSM (raster scanning method) mode. As shown in Figure 9, in the raster mode, all voxels which constitute the volume whose contains the microstructure are scanned. In case of CSM mode, only the voxels defining the surface of the microstructure are scanned. As a result, it took 3 hours or 13 minutes to manufacture the micro-bull using RSM and CSM mode respectively (Sun, 2003). Further information on the role played by trajectories can be found laser and photonics review (Park et al., 2009).

For applications where the objects have to be completely filled such as microlens, an additional UV exposure step is done. However cracks in the structure might occur to leading to a dramatic decrease of desired performance.

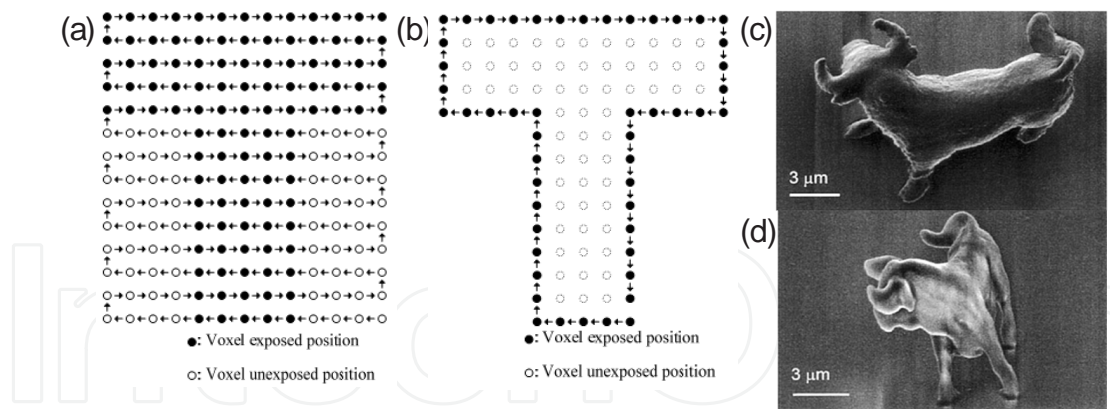


Figure 9. Two fabrication strategies based on scanning mode: a) Raster mode, b) Vector mode (or contour mode), c) and d) SEM images of a microbull structures using RSM and CSM respectively. Reproduced from reference Sun 2003.

4.2.2. Replication

To address the low-throughput of the method, LaFratta et al. have proposed to use TPS in tandem with soft lithography technique known as microtransfer molding (Xia et al. 1998). By this way, high-fidelity molds of structures with extremely high aspect ratios and large overhangs have been realized (LaFratta et al. 2004, Figure 10). Besides, in the frame of this work, more than ten replicas have been made from a single master without any significant deterioration of the resulting structures. Even if this technique have been applied to more complex structures such as arches or coils (LaFratta et al. 2006), a range of geometries or objects such as closed traps or micropumps are still impossible or currently too challenging to replicate using microtransfer molding. Finally, from our knowledge, no improvement or additional example of this technique has been recently reported in the literature, underlying the difficulties to separate the molder to the master without damage. Recent advances in soft lithography might facilitate the delivering step.

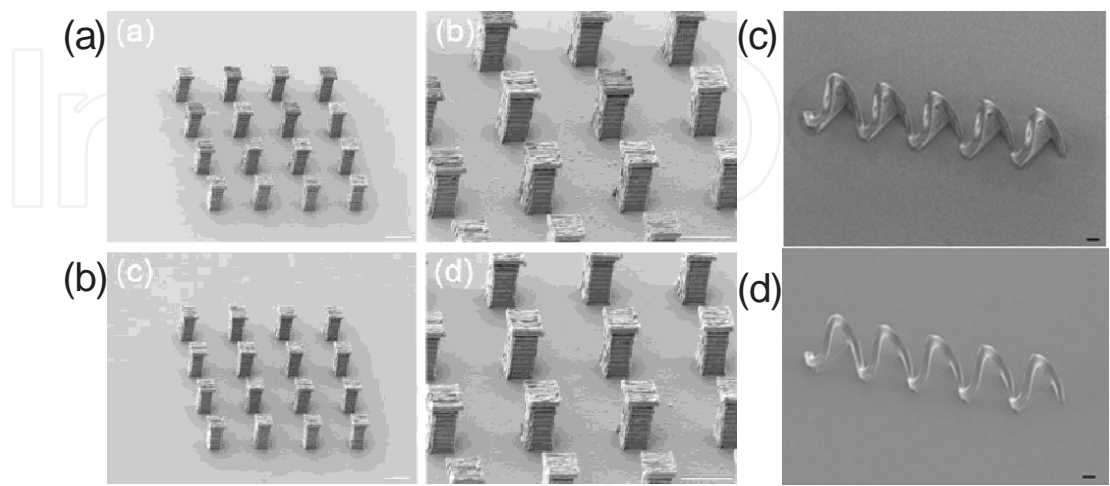


Figure 10. a) and b) SEM images of master and replica array of towers respectively, c) and d) SEM images of master and replica of coil respectively. Scale bars are 10 μm. Reproduced from reference LaFratta 2004 and 2006.

4.2.3. Multi-focal TPS

Another solution for boosting fabrication speed while avoiding geometric limitations associated with molding is the use of multi-focal strategy. This technical innovation has been first demonstrated by Kawata and coworkers in 2005 (Kato, 2005). By combining TPS with a microlens array, more than one hundred identical and individual 3D objects have been written simultaneously resulting in a two-order increase in the fabrication yield compared to single-beam TPS (Figure 11). In 2006, Kawata et al. succeed to write in parallel more than 700 hundred identical structures (Formanek, 2006) illustrating the high potential for large scale production.

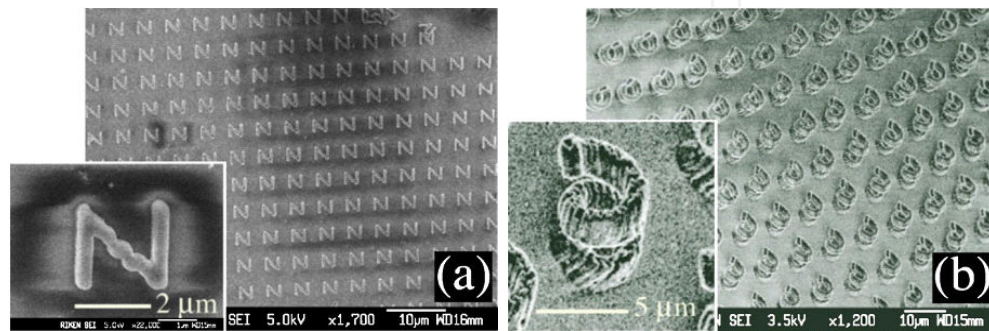


Figure 11. a) and b) examples of two- and three-dimensional fabrication by mean of microlens array.

Recently, Ritschdorff et al. proposed a more general approach of multi-focal TPS to allow parallel but independently writing of different objects (Ritschdorff et al. 2012). Indeed, until this work, advanced TPS based on multi-focal strategy was dedicated to the creation of identical replicas or to the fabrication of a single structure with many identical sub-units. In the frame of this recent work, a proof-of-concept has been illustrated with the construction of biocompatible networks by using two independent sub-beams. In order to control each beam separately, the main beam is directed through a dynamic mask (typically a spatial light modulator). To extend this appealing strategy to numerous parallel and independently sub-beam, high-power lasers are required. Additionally to the increase of the fabrication's speed, this work opens the doors to numerous and more flexible applications. For example, one could imagine making unlimited modifications into microfluidic systems, but more interestingly, generation of pattern with different exposure time will result to display gradients in chemical functionality, mechanical functionality or porosity which play a key role in tissue engineering.

However the promising potential of multi-focal TPS for speed up fabrication is quite obvious, two points have to be taken in consideration to use it as a tool in laboratory or industries. The first point concerns the use of an expensive amplified femtosecond laser in order to provide enough energy after each lens or dynamic mask. In addition, the laser beam intensity distribution has also to be perfectly controlled to deliver the same amount of energy for each lens and to fabricate uniform structures. It has to be mentioned that though this point may be a brake for scientific community, this is clearly not the case for its use in industry. A more serious issue with parallel fabrication is the precise control of alignment of the hundred forming laser beams with respect to the plan of the substrate. A tilt of less than 1° of the substrate will result

in the fabrication of inhomogeneous structures which is unacceptable from a metrology point of view in industries.

4.2.4. *Currently speed of TPS process*

In the literature, usual process speeds of several $100 \mu\text{m.s}^{-1}$ are reported with sub-100 nm resolution. More rarely, mm.s^{-1} can be reached while keeping a submicrometric resolution. Until recently, the fastest demonstration of microstructures with micrometric resolution has been realized by Fourkas's group by using a very sensitive photoinitiator (Kumi et al. 2010). In the frame of this work, speed of 1 cm.s^{-1} was reported.

Since march 2012, a 300-micrometer long model of a Formula 1 race car has been fabricated by TPS in only four minutes while keeping micrometric resolution. Thus spectacular result means that a process speed of 5 m.s^{-1} is involved, which is the same order of other laser process used in industry. A video of the construction can be found on the website of the Vienna University (Vienna, 2012). Unfortunately, certainly due to economic interests, little information can be freely accessed. According to their website, the increase in speed results from efforts from a chemical and mechanical point of view.

5. Conclusion and perspectives

After the pioneers works on TPS (Maruo, 1997), the research efforts were mainly focused on the synthesis of high efficient photoinitiators and materials in order to respectively speed up the writing process and to improve the mechanical, optical or chemical properties of the resulting 3D objects. Thanks to both the versatility of photopolymerizable systems and to the possibility to incorporate additional materials into the structures, TPS has attracted considerable attention over the past decade leading to enough mature technology. Indeed, despite the novelty of TPS, this is now daily used for broad range of applications such as creation of 3D components for microfluidic systems, tissue scaffolding, optical components, and so on. Besides, only 10 years after the first instance of 3D microstructures created by TPS, several companies have developed commercial 3D microfabrication set-ups which have supported the widespread of the technique in various research fields.

Recently, the rapid technical development of TPS provided much better structural resolution and high-throughput. The combination of all these improvements in a single commercial set-up will certainly boost the use of TPS in industry. From resolution point of view, the Abbe diffraction limit in optical lithography has been overcome by using and/or adapting a concept called STED originally from optical microscopy. The latter is already commercialized since 2005 by several well-known optical microscopy companies and is well expanded in life sciences. Interestingly, even if both in optical microscopy and lithography the diffraction limit has been beaten thanks to the STED principle, record for lateral spatial resolution in optical lithography (175 nm) is still far away from thus in optical microscopy (5.6 nm). In order to obtain comparable resolution, further investigations are required to enhance the comprehension of the photophysical and photochemical mechanism underlying the STED lithography.

In particularly, a better understanding will give a list of criteria for novel photoinitiators devoted to this promising technique.

Concerning the throughput of the technique, speed of 5 m.s^{-1} has been recently announced by an European consortium (march 2012). For comparison, this speed is quite close to those used in conventional process in microelectronics industry such as control or ablation process (10 to 50 m.s^{-1}). Such promising advances should allow overcome limit for mass production and consequently should reinforce the highly potential of TPS for industry.

To conclude, this technology opens up new perspectives in a wide range of applications such as rapid prototyping of micro- and nanofluidics, small-scale production of microoptics components, or 3D frameworks for cell biology. Finally, owing to its currently fast expansion and to the versatile science involved in all the chain, TPS appears as a fantastic and so appealing field of research for the next decades.

Acknowledgements

Agence Nationale pour la Recherche (ANR - Projects 2-PAGmicrofab ANR-BLAN-0815-03, NANOQUENCHING and NIR-OPTICS), CNRS and Région Alsace are gratefully acknowledged for financial supports.

Author details

Arnaud Spangenberg^{1*}, Nelly Hobeika¹, Fabrice Stehlin¹, Jean-Pierre Malval¹, Fernand Wieder¹, Prem Prabhakaran², Patrice Baldeck² and Olivier Soppera¹

*Address all correspondence to: arnaud.spangenberg@uha.fr

1 Institut de Science des Matériaux de Mulhouse, Mulhouse, France

2 Laboratoire de Spectrométrie Physique, Université Joseph-Fourier, Saint Martin d'Hères, France

References

- [1] Amato, L, Gu, Y, Bellini, N, Eaton, S. M, Cerullo, G, & Osellame, R. (2012). Integrated three-dimensional filter separates nanoscale from microscale elements in a microfluidic chip. *Lab on a Chip*, , 12, 1135-1142.
- [2] Becker, E. W, Ehrfeld, W, & Muenchmeyer, D. (1984). Accuracy of X-ray lithography using synchrotron radiation for the fabrication of technical separation nozzle ele-

- ments. Inst. Kernverfahrenstech., Kernforschungszent. Karlsruhe G.m.b.H., Karlsruhe, Fed.Rep.Ger., , 92.
- [3] Belfield, K. D, & Abdelrazzaq, F. B. (1997). a. Novel photoinitiated cationic copolymerizations of 4-methylene-2-phenyl-1,3-dioxolane. *Journal of Polymer Science Part A: Polymer Chemistry*, , 35, 2207-2219.
 - [4] Belfield, K. D, & Abdelrazzaq, F. B. (1997). b. Photoinitiated Cationic Crosslinking of 4-Methylene-2-phenyl-1,3-dioxolane with 2,2'-(1,4-Phenylene)bis-4-methylene-1,3-dioxolane. *Macromolecules*, , 30, 6985-6988.
 - [5] Belfield, K. D, Schafer, K. J, Liu, Y, Liu, J, Ren, X, & Stryland, E. W. V. (2000). Multi-photon-absorbing organic materials for microfabrication, emerging optical applications and non-destructive three-dimensional imaging. *Journal of Physical Organic Chemistry*, , 13, 837-849.
 - [6] Billone, P. S, Park, J. M, Blackwell, J. M, Bristol, R, & Scaiano, J. C. (2009). Two-Photon Acid Generation in Thin Polymer Films. Photoinduced Electron Transfer As a Promising Tool for Subwavelength Lithography. *Chemistry of Materials*, , 22, 15-17.
 - [7] Blanc, D, Pelissier, S, Saravanamuttu, K, Najafi, S. I, & Andrews, M. P. (1999). Self-processing of surface relief gratings in photosensitive hybrid sol-gel glasses. *Advanced Materials*, , 11, 1508-1511.
 - [8] Bückmann, T, Stenger, N, Kadic, M, Kaschke, J, Frölich, A, Kennerknecht, T, Eberl, C, Thiel, M, & Wegener, M. (2012). Tailored 3D Mechanical Metamaterials Made by Dip-in Direct-Laser-Writing Optical Lithography. *Advanced Materials*, , 24, 2710-2714.
 - [9] Burmeister, F, Zeitner, U. D, Nolte, S, & Tünnermann, A. (2012). High numerical aperture hybrid optics for two-photon polymerization. *Optics Express*, , 20, 7994-8005.
 - [10] Campbell, M, Sharp, D. N, Harrison, M. T, Denning, R. G, & Turberfield, A. J. (2000). Fabrication of photonic crystals for the visible spectrum by holographic lithography. *Nature*, , 404, 53-56.
 - [11] Cao, Y, Gan, Z, Jia, B, Evans, R, & Gu, M. (2011). High-photosensitive resin for super-resolution direct-laser-writing based on photoinhibited polymerization. *Optics Express*, , 19, 19486-19494.
 - [12] Cerrina, F. (1997). Application of X-rays to Nanolithography. *Proc. IEEE*, , 84, 644-651.
 - [13] Cumpston, B. H, Ananthavel, S. P, Barlow, S, Dyer, D. L, Ehrlich, J. E, Erskine, L. L, Heika, A. A, Kuebler, S. M, Lee, I, Mccord-maughon, Y. S, Qin, D, Rockel, J, Rumi, H, Wu, M, Marder, X. -L, Perry, S. R, & Two-photon, J. W. polymerization initiators for three-dimensional optical data storage and microfabrication. *Nature*, , 398, 51-54.
 - [14] Denk, W, Strickler, J, & Webb, W. W. (1990). Two-photon laser scanning fluorescence microscopy. *Science*, , 248, 73-76.

- [15] Devoe, R. J, Kalweit, H, Leatherdale, C. A, & Williams, T. R. (2002). Voxel shapes in two-photon microfabrication. *Proceeding of the SPIE*, , 4797, 310-316.
- [16] Dittrich, P. S, Tachikawa, K, & Manz, A. (2006). Micro total analysis systems. Latest advancements and trends. *Analytical Chemistry*, , 78, 3887-3908.
- [17] Emons, M, Obata, K, Binhammer, T, Ovsianikov, A, Chichkov, B, & Morgner, U. (2012). Two-photon polymerization technique with sub-50 nm resolution by sub-10 fs laser pulses. *Optical Materials Express*, , 2, 942-947.
- [18] Hell, S. W, Jakobs, S, & Kastrop, L. (2003). Imaging and writing at the nanoscale with focused visible light through saturable optical transitions. *Applied Physics A: Materials Science & Processing*, , 77, 859-860.
- [19] Fan, H. J, Werner, P, & Zacharias, M. (2006). Semiconductor Nanowires: From Self-Organization to Patterned Growth. *Small*, March 2006), , 2(700), 700-717.
- [20] Fischer, J, Von Freymann, G, & Wegener, M. (2010). The Materials Challenge in Diffraction-Unlimited Direct-Laser-Writing Optical Lithography. *Advanced Materials*, , 22, 3578-3582.
- [21] Fischer, J, Ergin, T, & Wegener, M. (2011). Three-dimensional polarization-independent visible-frequency carpet invisibility cloak. *Optics Letters*, , 36, 2059-2061.
- [22] Fischer, J, & Wegener, M. optical laser lithography beyond the diffraction limit. *Laser & Photonics Reviews*, DOI:10.1002/lpor.201100046.
- [23] Fischer, J, & Wegener, M. (2012b). Ultrafast Polymerization Inhibition by Stimulated Emission Depletion for Three-dimensional Nanolithography. *Advanced Materials*, , 24, OP65-OP69.
- [24] Formanek, F, Takeyasu, N, Tanaka, T, Chiyoda, K, Ishikawa, A, & Kawata, S. (2006). Three-dimensional fabrication of metallic nanostructures over large areas by two-photon polymerization. *Optics Express*, , 14, 800-809.
- [25] Goeppert-mayer, M. (1931). Über Elementarakte mit zwei Quantensprüngen, *Annalen der Physik*, , 401, 273-294.
- [26] Gonsalves, K. E, Wang, M, Lee, C. T, Yueh, W, Tapia-tapia, M, Batina, N, & Henderson, C. L. (2009). Novel chemically amplified resists incorporating anionic photoacid generator functional groups for sub-50-nm half-pitch lithograph. *J. Mater. Chem.* March 2009), , 19, 2797-2802.
- [27] Grotjohann, T, Testa, I, Leutenegger, M, Bock, H, Urban, N. T, Lavoie-cardinal, F, Willig, K. I, Eggeling, C, Jakobs, S, & Hell, S. W. (2011). Diffraction-unlimited all-optical imaging and writing with a photochromic GFP. *Nature*, , 478, 204-208.
- [28] Harke, B, Bianchini, P, Brandi, F, & Diaspro, A. (2012). Photopolymerization Inhibition Dynamics for Sub-Diffraction Direct Laser Writing Lithography. *Chemical Physical Chemistry*, , 13, 1429-1434.

- [29] Haske, W, Chen, V. W, Hales, J. M, Dong, W. T, Barlow, S, Marder, S. R, & Perry, J. W. (2007). nm feature sizes using visible wavelength 3-D multiphoton lithography. *Optics Express*, , 15, 3426-3436.
- [30] He, G. S, Tan, L. S, Zheng, Q, & Prasad, P. N. (2008). Multiphoton absorbing materials: Molecular designs, characterizations, and applications. *Chemical Reviews*, , 108, 1245-1330.
- [31] Hell, S. W, & Wichmann, J. (1994). Breaking the diffraction resolution limit by stimulated emission: stimulated emission depletion fluorescence microscopy. *Optics Letters*, , 19, 780-782.
- [32] Henzie, J, Barton, J. E, Stender, C. L, & Odom, T. W. (2006). Large-area nanoscale patterning: chemistry meets fabrication. *Accounts of Chemical Research*, January 2006), , 39(4), 249-257.
- [33] Im, S. G, Kim, B. S, Tenhaeff, W. E, Hammond, P. T, & Gleason, K. K. (2009). A directly patternable click-active polymer film via initiated chemical vapor deposition (iCVD). *Thin Solid Films*. January 2009), , 517(12), 3606-3611.
- [34] Iosin, M, Scheul, T, Nizak, C, Stephan, O, Astilean, S, & Baldeck, P. (2011). Laser microstructuring of three-dimensional enzyme reactors in microfluidic channels. *Microfluidics and Nanofluidics*, , 10, 685-690.
- [35] Jin, M, Malval, J. P, Versace, D. L, Morlet-savary, F, Chaumeil, H, Defoin, A, Allonas, X, & Fouassier, J. P. (2008). Two-photon absorption and polymerization ability of intramolecular energy transfer based photoinitiating systems. *Chemical Communications*, , 48, 6540-6542.
- [36] Kaiser, W, & Garrett, C. G. B. (1961). Two-photon excitation in $\text{CaF}_2\text{:Eu}^{2+}$. *Physical Review Letters*, , 7, 229-232.
- [37] Kato, J, Takeyasu, N, Adachi, Y, Sun, H. B, & Kawata, S. (2005). Multiple-spot parallel processing for laser micronanofabrication. *Applied Physics Letters*, , 86
- [38] Kawata, S, Sun, H. B, Tanaka, T, & Takada, K. (2001). Finer features for functional microdevices- Micromachines can be created with higher resolution using two-photon absorption. *Nature*, , 412, 697-698.
- [39] Klar, T. A, & Hell, S. W. (1999). Subdiffraction resolution in far-field fluorescence microscopy. *Optics Letters*, , 24, 954-956.
- [40] Klein, F, Richter, B, Striebel, T, Franz, C. M, Von Freymann, G, Wegener, M, & Bastmeyer, M. (2011). Two-Component Polymer Scaffolds for Controlled Three-Dimensional Cell Culture. *Advanced Materials*, , 23, 1341-1345.
- [41] Kodama, H. (1981). Automatic Method for fabricating a 3-dimensional plastic model with photo-hardening polymer. *Rev. Sci. Instrum.*, , 52, 1770-1773.

- [42] Kovacs, G. T. A, Maluf, N. I, & Petersen, K. E. (1998). Bulk micromachining of silicon. *Proceeding of the IEEE* , 86, 1536-1551.
- [43] Kumi, G, Yanez, C. O, Belfield, K. D, & Fourkas, J. T. (2010). High-speed multiphoton absorption polymerization: fabrication of microfluidic channels with arbitrary cross-sections and high aspect ratios. *Lab on a Chip* , , 10, 1057-1060.
- [44] LaFrattaC. N.; Baldacchini, T.; Farrer, R. A.; Fourkas, J. T.; Teich, M. C.; Saleh, B. E. A.; Naughton, M. J. ((2004). Replication of two-photon-polymerized structures with extremely high aspect ratios and large overhangs. *Journal of Physical Chemistry B* , , 108, 11256-11258.
- [45] LaFrattaC. N. ; Li, L. J.; Fourkas, J. T. ((2006). Soft-lithographic replication of 3D microstructures with closed loops. *Proceedings of the National Academy of Sciences of the United States of America* , , 103, 8589-8594.
- [46] Lee, J-H, Singer, J. P, & Thomas, E. L. (2012). Micro-/Nanostructured Mechanical Metamaterials. *Advanced Materials* , , 24, 4782-4810.
- [47] Lewis, J. A, & Gratson, G. M. (2004). Direct Writing in Three Dimensions. *Materials Today* , , 7, 32-39.
- [48] Li, C, Luo, L, Wang, S, Huang, W, Gong, Q, Yang, Y, & Feng, S. (2001). Two-photon microstructure-polymerization initiated by a coumarin derivative/iodonium salt system. *Chemical Physics Letters* , , 340, 444.
- [49] Li, X, Zhao, Y, Wu, J, Shi, M, & Wu, F. (2007). Two-photon photopolymerization using novel asymmetric ketocoumarin derivatives. *Journal of Photochemistry and Photobiology A: Chemistry* , , 190, 22-28.
- [50] Li, L. J, Gattass, R. R, Gershgoren, E, Hwang, H, & Fourkas, J. T. (2009). Achieving $\lambda/20$ Resolution by One-Color Initiation and Deactivation of Polymerization. *Science* , 324, 910-913.
- [51] Lu, Y, Hasegawa, F, Goto, T, Ohkuma, S, Fukuhara, S, Kawazu, Y, Totani, K, Yamashita, T, & Watanabe, T. (2004). Highly sensitive measurement in two-photon absorption cross section and investigation of the mechanism of two-photon-induced polymerization. *Journal of Luminescence* , , 110, 1-10.
- [52] Lu, W. E, Dong, X. Z, Chen, W. Q, Zhao, Z. S, & Duan, X. M. (2011). Novel photoinitiator with a radical quenching moiety for confining radical diffusion in two-photon induced photopolymerization. *Journal of Materials Chemistry* , , 21, 5650-5659.
- [53] Malval, J. P, Jin, M, Morlet-savary, F, Chaumeil, H, Defoin, A, Soppera, O, Scheul, T, Bouriau, M, & Baldeck, P. L. (2011). Enhancement of the Two-Photon Initiating Efficiency of a Thioxanthone Derivative through a Chevron-Shaped Architecture. *Chemistry of Materials* , , 23, 3411-3420.

- [54] Martineau, C, Anemian, R, Andraud, C. W, Bouriau, I, & Baldeck, M. P. L. ((2000). Efficient initiators for two-photon induced polymerization in the visible range. *Chemical Physics Letters*, , 362, 291-295.
- [55] Maruo, S, Nakamura, O, & Kawata, S. (1997). Three-dimensional microfabrication with two-photon-absorbed photopolymerization. *Optics Letters*, , 22, 132-134.
- [56] Maruo, S, & Ikuta, K. (2002). Submicron stereolithography for the production of freely movable mechanisms by using single-photon polymerization. *Sensors and Actuators, A: Physical*, A100, , 70-76.
- [57] Maruo, S, & Inoue, H. (2006). Optically driven micropump produced by three-dimensional two-photon microfabrication. *Applied Physics Letters*, , 89, 144101.
- [58] Mcleod, R. R, Kowalski, B. A, & Cole, M. C. (2010). Two-color photo-initiation/inhibition lithography. *Proceeding of the SPIE*, , 7591, 759102-759107.
- [59] Moore, G. E. (1965). Cramming More Components Onto Integrated Circuits. *Electronics*, April 1965), , 38(8), 114-117.
- [60] Ovsianikov, A, Viertl, J, Chichkov, B, & Oubaha, M. MacCraith, B.; Sakellari, L.; Giakoumaki, A.; Gray, D.; Vamvakaki, M.; Farsari, M.; Fotakis, C. ((2008). Ultra-Low Shrinkage Hybrid Photosensitive Material for Two-Photon Polymerization Microfabrication. *ACS Nano*, , 2, 2257-2262.
- [61] Pao, Y-H, & Rentzepis, P. M. (1965). Laser-induced production of free radicals in organic compounds. *Applied Physics Letters*, , 6, 93-95.
- [62] Park, S. H, Yang, D. Y, & Lee, K. S. (2009). Two-photon stereolithography for realizing ultraprecise three-dimensional nano/microdevices. *Laser & Photonics Reviews*, , 3, 1-11.
- [63] Passinger, S, Saifullah, M. S. M, Reinhardt, C, Subramanian, K. R. V, Chichkov, B. N, & Welland, M. E. (2007). Direct 3D Patterning of TiO₂ Using Femtosecond Laser Pulses. *Advanced Materials*, , 19, 1218-1221.
- [64] Quake, S. R, & Scherer, A. (2000). From Micro- to Nanofabrication with Soft Materials. *Science*, , 290, 1536-1540.
- [65] Reyes, D. R, Iossifidis, D, Auroux, P, & Manz, A. A. ((2002). Micro total analysis systems. 1. Introduction, theory, and technology. *Analytical Chemistry*, , 74, 2623-2636.
- [66] Ridaoui, H, Wieder, F, Ponche, A, & Soppera, O. (2010). Direct ArF laser photopatterning of metal oxide nanostructures prepared by the sol-gel route. *Nanotechnology*, January 2010), , 21(6), 065303.
- [67] Rill, M. S, Plet, C, Thiel, M, Staude, I, Von Freymann, G, Linden, S, & Wegener, M. (2008). Photonic metamaterials by direct laser writing and silver chemical vapour deposition. *Nature Materials*, , 7, 543-546.

- [68] Ritschdorff, E. T, Nielson, R, & Shear, J. B. (2012). Multi-focal multiphoton lithography. *Lab on a Chip*, , 12, 867-871.
- [69] Rittweger, E, Han, K. Y, Irvine, S. E, Eggeling, C, & Hell, S. W. (2009). STED microscopy reveals crystal colour centres with nanometric resolution. *Nature Photonics*, , 3, 144-147.
- [70] Rumi, M, Ehrlich, J. E, Heikal, A, Perry, J. W, Barlow, S, Hu, Z. Y, Mccord-maughon, D, Parker, T. C, Rockel, H, Thayumanavan, S, Marder, S. R, Beljonne, D, & Bredas, J. L. (2000). Structure-property relationships for two-photon absorbing chromophores: Bis-donor diphenylpolyene and bis(styryl)benzene derivatives. *Journal of the American Chemical Society*, , 122, 9500-9510.
- [71] Sakellari, I, Kabouraki, E, Gray, D, Purlys, V, Fotakis, C, Pikulin, A, Bityurin, N, Vamvakaki, M, & Farsari, M. (2012). Diffusion-Assisted High-Resolution Direct Femtosecond Laser Writing. *ACS Nano*, , 6, 2302-2311.
- [72] Scott, T. F, Kowalski, B. A, Sullivan, A. C, Bowman, C. N, & Mcleod, R. R. (2009). Two-Color Single-Photon Photoinitiation and Photoinhibition for Subdiffraction Photolithography. *Science*, , 324, 913-919.
- [73] Shevchenko, E. V, Talapin, D. V, Rogach, A. L, Kornowski, A, Haase, M, & Weller, H. (2002). Colloidal synthesis and self-Assembly of CoPt₃ nanocrystals. *Journal of the American Chemical Society*, , 104, 11480-11485.
- [74] Shukla, S, Vidal, X, Furlani, E. P, Swihart, M. T, Kim, K. T, Yoon, Y. K, Urbas, A, & Prasad, P. N. (2011). Subwavelength Direct Laser Patterning of Conductive Gold Nanostructures by Simultaneous Photopolymerization and Photoreduction. *ACS Nano*, , 5, 1947-1957.
- [75] Soppera, O, Croutxe-barghorn, C, & Lougnot, D. J. (2001). New insights into photoinduced processes in hybrid sol-gel glasses containing modified titanium alkoxides. *New Journal of Chemistry*, , 25, 1006-1014.
- [76] Spangenberg, A, Malval, J. P, Akdas-kilig, H, Fillaut, J. L, Stehlin, F, Hobeika, N, Morlet-savary, F, & Soppera, O. (2012). Enhancement of Two-Photon Initiating Efficiency of a 4,4'-Diaminostyryl-2,2'-bipyridine Derivative Promoted by Complexation with Silver Ions. *Macromolecules*, , 45, 1262-1268.
- [77] Steidl, L, Jhaveri, S. J, Ayothi, R, Sha, J, McMullen, J. D, Ng, S. Y. C, Zipfel, W. R, Zentel, R, & Ober, C. K. (2009). Non-ionic photo-acid generators for applications in two-photon lithography. *Journal of Materials Chemistry*, , 19, 505.
- [78] Stocker, M. P, Li, L. J, Gattass, R. R, & Fourkas, J. T. (2010). Multiphoton photoresists giving nanoscale resolution that is inversely dependent on exposure time. *Nature Chemistry*, , 3, 223-227.

- [79] Sun, H. B, & Kawata, S. (2003). Two-photon laser precision microfabrication and its applications to micro-nano devices and systems. *Journal of Lightwave Technology*, , 21, 624-633.
- [80] Sun, H. B, Tanaka, T, & Kawata, S. (2002). Three-dimensional focal spots related to two-photon excitation. *Applied Physics Letters*, , 80, 3673-3675.
- [81] Sun, Q, Juodkazis, S, Murazawa, N, Mizeikis, V, & Misawa, H. (2010). Freestanding and movable photonic microstructures fabricated by photopolymerization with femtosecond laser pulses. *Journal of Micromechanics and Microengineering*, , 20, 035004.
- [82] Takada, K, Sun, H-B, & Kawata, S. (2005). Improved spatial resolution and surface roughness in photopolymerization-based laser nanowriting. *Applied Physics Letters*, , 86, 071122.
- [83] Vienna (2012). <http://amt.tuwien.ac.at/projekte/2pp/>.
- [84] Wang, I, Bouriau, M, Baldeck, P. L, Martineau, C, & Andraud, C. (2002). Three-dimensional microfabrication by two-photon-initiated polymerization with a low-cost microlaser. *Optics Letters*, , 27, 1348-1350.
- [85] West, J, Becker, M, Tombrink, S, & Manz, A. (2008). Micro total analysis systems: Latest achievements. *Analytical Chemistry*, , 80, 4403-4419.
- [86] Wolf, T. J. A, Fischer, J, Wegener, M, & Unterreiner, A-N. (2011). Pump-probe spectroscopy on photoinitiators for stimulated-emission-depletion optical lithography. *Optics Letters*, , 36, 3188-3190.
- [87] Wu, E, Strickler, J. H, Harrell, W. R, & Webb, W. W. (1992). Two-photon lithography for microelectronic application. *Proc. SPIE* , 1674, 776-782.
- [88] Xia, Y, & Whitesides, G. M. (1998). Soft Lithography. *Angewandte Chemie International Edition*, , 37, 550-575.
- [89] Xia, R, Malval, J. P, Jin, M, Spangenberg, A, Wan, D, Pu, H, Vergote, T, Morlet-savary, F, Chaumeil, H, Baldeck, P, Poizat, O, & Soppera, O. (2012). Enhancement of Acid Photogeneration Through a Para-to-Meta Substitution Strategy in a Sulfonium-based Alkoxystilbene Designed for Two-Photon Polymerization. *Chemistry of Materials*, , 24, 237-244.
- [90] Xing, J. F, Dong, X. Z, Chen, W. Q, Duan, X. M, Takeyasu, N, Tanaka, T, & Kawata, S. (2007). Improving spatial resolution of two-photon microfabrication by using photoinitiator with high initiating efficiency. *Applied Physics Letters*, , 90, 131106.
- [91] Yanez, C. O, Andrade, C. D, & Belfield, K. D. (2009). Characterization of novel sulfonium photoacid generators and their microwave-assisted synthesis. *Chemical Communication*, , 7, 827.

- [92] Zhang, X, Yu, X. Q, Sun, Y, Wu, Y, Feng, Y, Tao, X, & Jiang, M. (2005). Synthesis and nonlinear optical properties of a new D- π -A two-photon photopolymerization initiator. *Material Letters*, , 59, 3485-3488.
- [93] Zhou, W, Kuebler, S. M, Braun, K. L, Yu, T, Cammack, J. K, Ober, C. K, Perry, J. W, & Marder, S. R. (2002). An efficient two-photon-generated photoacid applied to positive-tone 3D microfabrication. *Science*, , 296, 1106.

